IEICE TRANSACTIONS

on Electronics

DOI:10.1587/transele.2024REP0004

Publicized:2024/09/20

This advance publication article will be replaced by the finalized version after proofreading.

A PUBLICATION OF THE ELECTRONICS SOCIETY

The Institute of Electronics, Information and Communication Engineers
Kikai-Shinko-Kaikan Bldg., 5-8, Shibakoen 3chome, Minato-ku, TOKYO, 105-0011 JAPAN

PAPER *Special Section on Recent Progress in Electromagnetic Theory and Its Application*

Analysis of optical resonator with waveguide discontinuities constructed by two-dimensional MDM plasmonic waveguide

Yoshihiro NAKA[†a)], ***Member***, **Masahiko NISHIMOTO**[††], ***and*** **Mitsuhiro YOKOTA**[†], ***Senior Members***

SUMMARY An optical resonator with two waveguide discontinuities constructed by a metal-dielectric-metal plasmonic waveguide has been analyzed using the finite-difference time-domain (FD-TD) method with the piecewise linear recursive convolution (PLRC) method. The waveguide discontinuity has been expressed as an equivalent transmission line circuit whose circuit parameters are estimated from the reflection coefficients analyzed by the FD-TD method. We have confirmed the validity of the circuit configuration because the reflection characteristics of the equivalent circuit with the circuit parameters agree with those of the FD-TD method. Next, we have analyzed a resonator structure with two waveguide discontinuities and shown that the equivalent circuit gives a good approximation for the structure with a large difference in waveguide width at the discontinuities, in which conventional equivalent circuits had large errors.

key words: *plasmonic waveguide, resonator, waveguide discontinuity, transmission line circuit, FD-TD method, PLRC method*

1. Introduction

A plasmonic waveguide that utilize surface plasmon polaritons (SPPs) propagating along a dielectric-metal interface can narrow the waveguide width to several tens of nanometers, which exceeds the diffraction limit of light[1]–[3]. Furthermore, since it can be fabricated using existing CMOS processes, it is expected that highly efficient submicron size optical circuit elements based on silicon photonics technology[4]–[6] can be realized[1]–[3], [7]–[17]. Light is strongly confined in the plasmonic waveguide because it is localized along the dielectric-metal interface and there is little light penetration into a metal cladding layer. Therefore, characteristics of the plasmonic waveguides are similar to TEM waves propagating in a parallel plate waveguide. Many studies have been reported to utilize this property to represent the plasmonic waveguides with equivalent transmission line circuits[1], [18], [19].

We have expressed a symmetric waveguide discontinuity constructed by two-dimensional metal-dielectric-metal (MDM) plasmonic waveguides shown in Fig. 1 (a) as an equivalent transmission-line circuit shown in Fig. 1(b)[20]. The transmission characteristics of a resonator structure with two waveguide discontinuities analyzed by the finite-difference time-domain (FD-TD) method and the equivalent circuit were compared. The results showed that the transmission-line circuit model gives a good approximation for a small difference in waveguide width at the discontinuities, however, there are large errors in a resonant wavelength and an optical power transmittance for a large difference in waveguide width at the discontinuities[20]. It is considered that the errors are caused because the waveguide discontinuity was expressed only as a characteristic impedance mismatch, which does not take into account a phase change. An equivalent circuit has been modified to consider the phase change at a waveguide discontinuity in [21]. In addition, an equivalent circuit considering the effect of the strong waveguide dispersion shown in Fig. 1 (c) has been proposed in [18], but the characteristics were analyzed only for a monochromatic wavelength in [18]. However, in optical devices for the wavelength-division multiplexing system, it is important to consider the effect of both material dispersion and waveguide dispersion. Therefore, this paper investigates the effect of both dispersions by analyzing the wavelength characteristics of a modified equivalent circuit of a waveguide discontinuity.

In this paper, we employ the modified circuit[18] shown in Fig. 1 (c) for the symmetric waveguide discontinuity. The circuit parameters are estimated from reflection coefficients

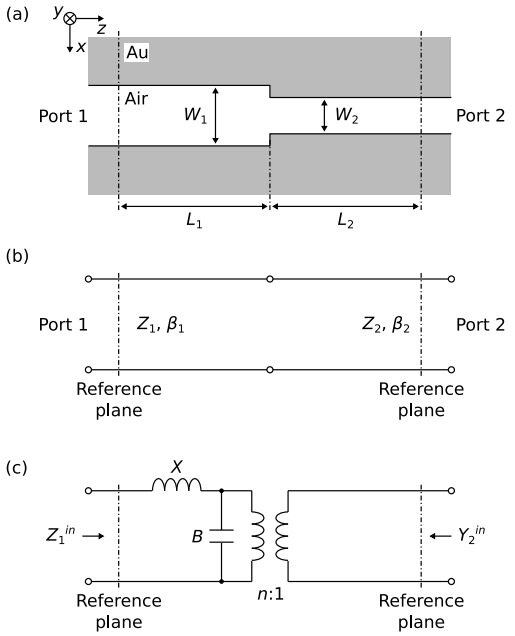

Fig. 1 Discontinuity of 2D MDM plasmonic waveguide. (a) waveguide structure, (b) equivalent transmission-line circuit, (c) modified equivalent transmission-line circuit.

[†]The authors are with University of Miyazaki, Miyazaki-shi, 889-2192 Japan.

[††]The author is with Kumamoto University, Kumamoto-shi, 860-8555 Japan.

a) E-mail: ynaka@cc.miyazaki-u.ac.jp

analyzed by the FD-TD method. We confirm reflection characteristics of the modified equivalent circuit agree with those of the FD-TD method. Next, the modified equivalent circuit is applied to the resonator structure with two waveguide discontinuities. The results show that the equivalent circuit gives a good approximation for the structure with a large difference in waveguide width at the discontinuities.

2. Formulation of Problems

We consider a two-dimensional MDM plasmonic waveguides constructed by gold and air as shown in Fig. 1 (a). The MDM plasmonic waveguide used here has cladding layers of gold which is low-loss for infrared light, and a waveguide layer of air whose refractive index is 1.0. Two waveguides with different widths W_1, W_2 are connected. The gold is dispersive media and it has a negative permittivity for infrared and visible light[22], [23]. The method of solution is the FD-TD method with the piecewise linear recursive convolution (PLRC) method[24] for dispersive media. The computational zone is surrounded by the perfectly matched layers (PMLs)[25], [26] which are used as the absorbing boundary condition.

The dielectric constant of gold in the infrared wavelengths is estimated by the Drude model[22] as follows:

$$\varepsilon_r(f) = 1 - \frac{f_p^2}{f^2 + j\dfrac{f}{\tau}} \tag{1}$$

where f, $f_p = 1.38 \times 10^{16}$ Hz and $\tau = 9.3 \times 10^{-15}$ s are frequency, plasma frequency and relaxation time, respectively. The dielectric constant for infrared light has dispersibility and its imaginary part causes the optical loss. The polarization of the incident wave is transverse magnetic (TM) mode (H_y, E_x, E_z) because the MDM plasmonic waveguide has no surface plasmon polariton (SPP) mode for transverse electric (TE) mode. The grid cell sizes of $\delta = \delta x = \delta z = 2.5$ nm, and the time step of $c\delta t = 0.625\delta$ are used.

The MDM plasmonic waveguide can be expressed by a transmission-line circuit[27], [28] as shown in Fig. 1 (b) where Z_i and β_i ($i = 1, 2$) are the characteristic impedance and propagation constant for waveguide i, respectively. The mode field profile in the core can be regarded as constant when the incident wavelength λ is sufficiently large with respect to the waveguide width W_i. In addition, the penetration depth of the evanescent field in the cladding becomes small when the absolute value of the dielectric constant of the metal in the cladding $|\varepsilon_{\text{metal}}|$ is sufficiently larger than that of the dielectric in the core $\varepsilon_{\text{diel}}$. When these two conditions ($W_i \ll \lambda$ and $|\varepsilon_{\text{metal}}| \gg \varepsilon_{\text{diel}}$) are satisfied, the TM mode propagating in the MDM plasmonic waveguide can be approximated to the TEM mode propagating in the parallel perfect conductor plate waveguide[1], [19], which has the characteristic impedance as follows:

$$Z_i = \frac{\beta_i}{\omega\varepsilon_{\text{diel}}} W_i \tag{2}$$

where ω is angular frequency of the incident wave. The propagation constant β_i is calculated by numerically solving the dispersion eigenvalue equation for TM_0 mode of the two-dimensional MDM plasmonic waveguide[29]. The propagation constant β_i is a complex number because an MDM plasmonic waveguide has a propagation loss due to the material loss of a metal.

In this study, the circuit shown in Fig. 1 (c) is employed as the equivalent transmission-line circuit for the waveguide discontinuity[18]. In order to take into account the changes in phase, the circuit consists of a susceptance B, a reactance X, and a transformer with a transformation ratio n. When the equivalent circuit is normalized by the characteristic impedance Z_1 of the waveguide at port 1, the input impedance Z_1^{in} seen from port 1 and the input admittance Y_2^{in} seen from port 2 are given as follows:

$$Z_1^{in} = jX + \frac{1}{jB + n^{-2}} \tag{3}$$

$$Y_2^{in} = \left(\frac{1}{1 + jX} + jB\right) n^2 \tag{4}$$

From Eqs. (3) and (4), the circuit parameters are obtained[18] by

$$Bn^2 = \frac{\text{Im}\left(Y_2^{in}\right) + \text{Re}\left(Y_2^{in}\right)\text{Im}\left(Z_1^{in}\right)}{1 - \text{Re}\left(Y_2^{in}\right)\text{Re}\left(Z_1^{in}\right)} \tag{5}$$

$$X = \frac{\text{Im}\left(Z_1^{in}\right) + \text{Re}\left(Z_1^{in}\right)\text{Im}\left(Y_2^{in}\right)}{1 - \text{Re}\left(Y_2^{in}\right)\text{Re}\left(Z_1^{in}\right)} \tag{6}$$

$$n^2 = \text{Re}\left(Y_2^{in}\right)\left(1 + X^2\right) \tag{7}$$

On the other hand, Z_1^{in} and Y_2^{in} are also obtained from the current reflection coefficients corresponding to the magnetic field reflection coefficients S_{11} and S_{22} of the circuit as follows:

$$Z_1^{in} = -\frac{S_{11} - 1}{S_{11} + 1} \tag{8}$$

$$Y_2^{in} = \frac{1 + S_{22}}{1 - S_{22}} \tag{9}$$

Therefore, the equivalent circuit parameters B, X, and n can be determined from S_{11} and S_{22} of the waveguide discontinuity obtained by the FD-TD method which are calculated by the complex Fourier transform of a pulse response. The reflected field $\psi^-(t)$ in the input waveguide from the discontinuity is obtained by subtracting the incident field from the total field. The complex Fourier-transformed reflected field Ψ^- in the input waveguide at the reference plane at z_0, whose propagation length is $2L_1$, and the reference field Ψ^+_{ref} propagating in the waveguide with the same width as the input waveguide and length $2L_1$ are expressed by

$$\Psi^-(z_0) = \Psi^+_{\text{ref}}(z_0) S_{11} e^{-j2\beta_1 L_1} \tag{10}$$

$$\Psi^+_{\text{ref}}(z_0 + 2L_1) = \Psi^+_{\text{ref}}(z_0) e^{-j2\beta_1 L_1} \tag{11}$$

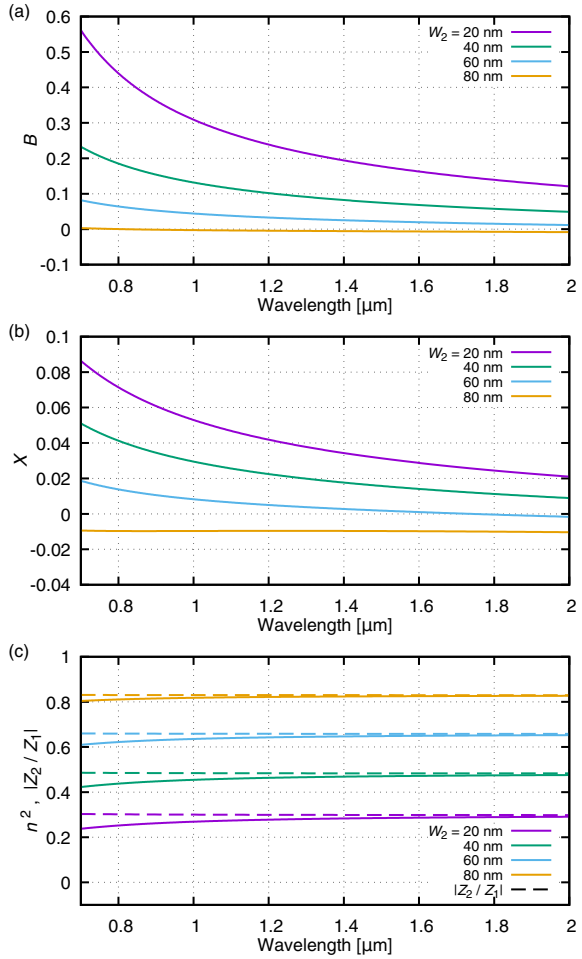

Fig. 2 Wavelength dependencies of the equivalent circuit parameters (a) B, (b) X, and (c) n^2 calculated from the magnetic field reflection coefficient S_{11} and S_{22} of the waveguide discontinuities analyzed by the FD-TD method. The waveguide width of the port 1 is $W_1 = 100$ nm.

From these equations the reflection coefficient at the discontinuity is obtained by

$$S_{11} = \frac{\Psi^{-}(z_0)}{\Psi^{+}_{\mathrm{ref}}(z_0 + 2L_1)} \tag{12}$$

S_{22} is obtained in the same manner.

3. Numerical Results

Figure 2 shows the wavelength dependencies of the equivalent circuit parameters B, X, and n^2 of the symmetric waveguide discontinuity for different waveguide widths W_2 of port 2, where the width $W_1 = 100$ nm of port 1 is fixed. The magnetic field reflection coefficients S_{11} and S_{22} are obtained by the FD-TD method. The plasmonic waveguide is a single-mode waveguide in which only the fundamental mode propagates in this wavelength range and waveguide width. In addition, there are no higher-order modes because the structure is symmetric. As shown in Fig. 2 (a) and (b), the greater the difference in waveguide width, the greater the

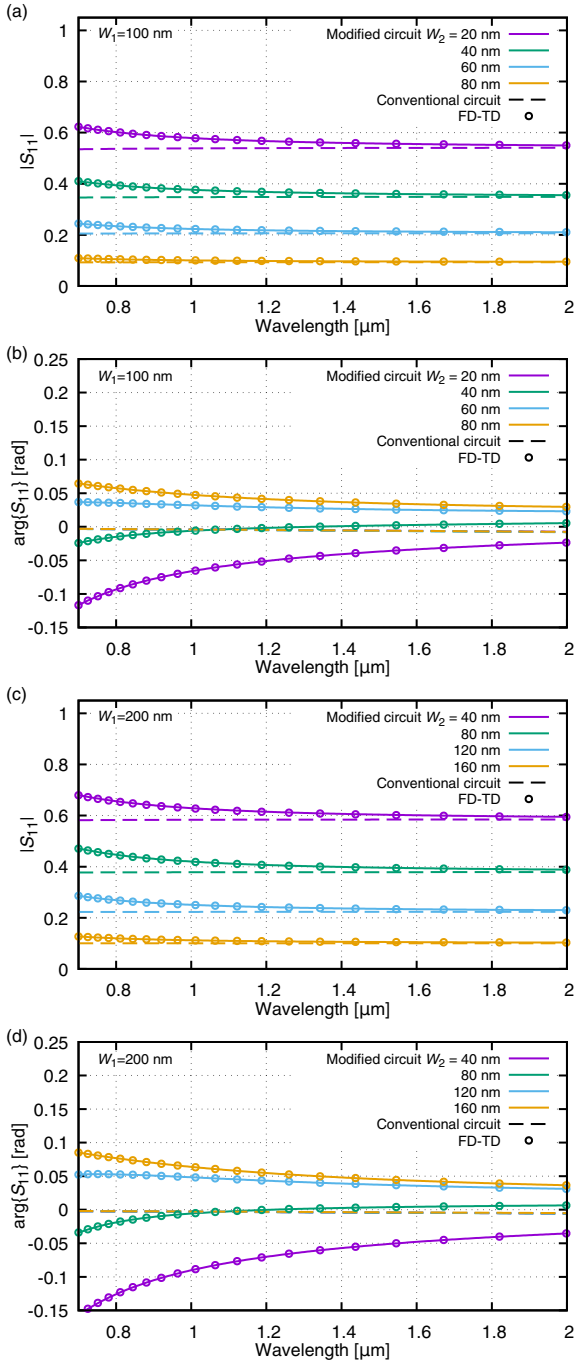

Fig. 3 Wavelength dependencies of magnetic field reflection coefficient S_{11} of the equivalent transmission-line circuit. (a)(c) Magnitude, (b)(d) Phase. The waveguide widths of the port 1 are (a)(b)$W_1 = 100$ nm and (c)(d)200 nm, respectively.

values of susceptance B and reactance X, and the greater their wavelength dependence. The square of the transformation ratio n^2 shown in Fig.2 (c) corresponds to the ratio of the characteristic impedances of port 1 and port 2 in the equivalent circuit. The ratio of characteristic impedance $|Z_2/Z_1|$ obtained by Eq. (2) is shown in the figure for comparison. While there is almost no wavelength dependence of

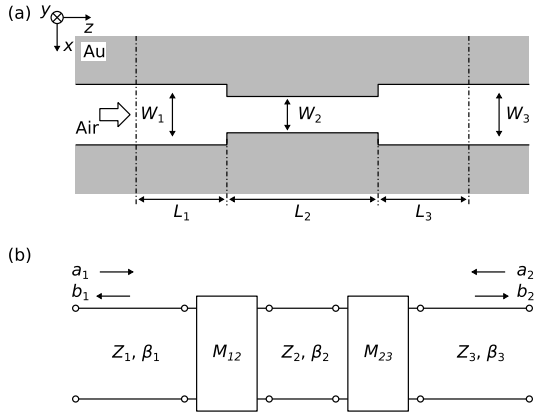

Fig. 4 2D MDM plasmonic waveguide with resonator structure. (a) waveguide structure, (b) equivalent transmission-line circuit.

$|Z_2/Z_1|$, the value of n^2 obtained from S_{11} and S_{22} analyzed by the FD-TD method decreases as the wavelength becomes shorter. As the difference in waveguide width increases, the wavelength dependence of n^2 also increases.

Figure 3 shows the spectra of the magnetic field reflection coefficients S_{11} of the modified equivalent circuit of the waveguide discontinuity with the parameters in Fig. 2. For comparison, the results of the conventional equivalent circuit in Fig. 1 (b) and the FD-TD method are also shown in the figure. The waveguide widths of port 1 are (a)(b) $W_1 = 100$ nm and (c)(d) 200 nm, respectively. It is confirmed that the modified equivalent circuit represents the waveguide discontinuity because the results of the modified equivalent circuit agree with those of the FD-TD method. In the conventional equivalent circuit, the wavelength dependence of both amplitude and phase is very small, and the difference from the results of the FD-TD method increases as the difference in waveguide width increases. Comparing the figures (a),(b) and (c),(d), even if the width ratio W_2/W_1 of the input and output waveguides is the same, there is a large difference in both amplitude and phase due to the strong dispersion of the effective index of the plasmonic waveguide in the wavelength range.

The resonator structure shown in Fig. 4, which connects two waveguide discontinuities, is then analyzed based on these results. In the transmission line circuit shown in Fig. 4 (b), the incident and reflected waves a_i and b_i, where i is the port number, are related by the transmission matrix (T-matrix) $\boldsymbol{T}$[30].

$$\begin{pmatrix} b_1 \\ a_1 \end{pmatrix} = \boldsymbol{T} \begin{pmatrix} a_2 \\ b_2 \end{pmatrix}, \ \boldsymbol{T} = \begin{pmatrix} T_{11} & T_{12} \\ T_{21} & T_{22} \end{pmatrix} \tag{13}$$

The T-matrix of the circuit is calculated by

$$\boldsymbol{T} = \boldsymbol{\Phi}_1 \boldsymbol{M}_{12} \boldsymbol{\Phi}_2 \boldsymbol{M}_{23} \boldsymbol{\Phi}_3 \tag{14}$$

where $\boldsymbol{\Phi}_i$ are the T-matrices described the phase shift in the waveguide i which are expressed by

$$\boldsymbol{\Phi}_i = \begin{pmatrix} e^{-j\beta_i L_i} & 0 \\ 0 & e^{j\beta_i L_i} \end{pmatrix} \tag{15}$$

and $\boldsymbol{M}_{i,j}$ are also the T-matrices described the modified equivalent circuit of the waveguide discontinuity between waveguide i and j shown in Fig. 1 (c). First, the circuit is represented by the scattering matrix (S-matrix), which is then converted to the T-matrix as follows:

$$\boldsymbol{M}_{i,j} = \frac{1}{2n} \begin{pmatrix} z_1 & z_2 \\ z_2^* & z_1^* \end{pmatrix} \tag{16}$$

where

$$z_1 = (1 - XB)n^2 + 1 - j(X + n^2 B) \tag{17}$$

$$z_2 = (1 - XB)n^2 - 1 + j(X - n^2 B) \tag{18}$$

and $*$ denotes the complex conjugate. The T-matrix (14) can be converted to the S-matrix

$$\boldsymbol{S} = \begin{pmatrix} S_{11} & S_{12} \\ S_{21} & S_{22} \end{pmatrix} = \frac{1}{T_{22}} \begin{pmatrix} T_{12} & T_{11}T_{22} - T_{12}T_{21} \\ 1 & -T_{21} \end{pmatrix} \tag{19}$$

The reflection coefficient of the input port and the transmission coefficient to the output port are obtained from S_{11} and S_{21}, respectively. Figure 5 shows optical power transmission and reflection spectra of the resonator structure for different narrow waveguide width W_2. The length of the narrow waveguide L_2 is 600 nm and 650 nm for input and output waveguide widths $W_1 = W_3 = 100$ nm and 200 nm, respectively. The distance between the reference planes ($L_1 + L_2 + L_3$) is 2 μm. From the figures, we can see that the insertion loss of the resonator structure increases as the waveguide width W_2 becomes narrower. This is because the propagation loss increases as the waveguide width decreases in an MDM plasmonic waveguide[20]. The resonant wavelength, the transmittance, and the reflectance of the modified circuit for large difference in waveguide width at the waveguide discontinuities are close to those of the FD-TD method. On the other hand, the difference in those of the conventional circuit and the FD-TD method is large for large differences in a waveguide width at the discontinuities. The relative error of the resonant wavelength by the modified equivalent circuit to that by the FD-TD method for several lengths L_2 of the narrow waveguide is shown in Fig. 6. We can find that the error is larger at longer wavelengths and shorter L_2. The optical length in a narrow waveguide becomes shorter at longer wavelengths because the effective index becomes smaller at longer wavelengths in an MDM plasmonic waveguide[29]. Therefore, both indicate that the error is larger when the optical length between the discontinuities is shorter. This may be due to the influence of the coupling of higher-order non-propagating modes that occur at the discontinuities because the equivalent circuit employed here considers only a fundamental mode[18].

4. Conclusion

We have analyzed a optical resonator structure with two waveguide discontinuies constructed by a two-dimensional MDM plasmonic waveguide by using the FD-TD method

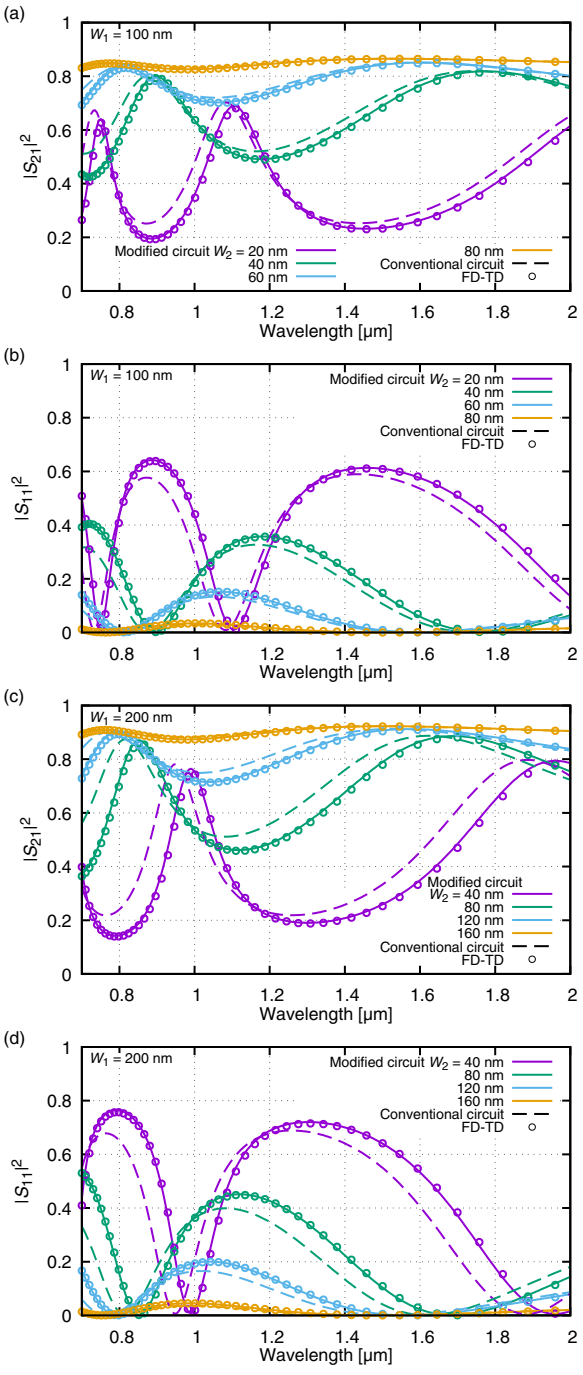

Fig. 5 Optical power (a)(c) transmission and (b)(d) reflection spectra of the resonator structure for different narrow waveguide width W_2. The waveguide width of the input / output waveguide and the length of the narrow waveguide are (a)(b) $W_1 = W_3 = 100$ nm, $L_2 = 600$ nm and (c)(d) $W_1 = W_3 = 200$ nm, $L_2 = 650$ nm, respectively. Solid lines, dashed lines, and circles are results of modified equivalent circuit, conventional equivalent circuit, and FD-TD method, respectively.

with the PLRC method. First, we have expressed the waveguide discontinuity as an equivalent transmission-line circuit that takes into account the changes in phase. The circuit parameters were estimated from reflection coefficients analyzed by the FD-TD method. From the reflection characteristics of the waveguide discontinuity, we have confirmed that the modified equivalent circuit represents the waveguide discontinuity because the results of the modified equivalent circuit agree with those of the FD-TD method. Next, the modified circuit has been applied to the resonator structure with two waveguide discontinuities. The reflectance and the transmittance spectra have shown that the modified circuit gives a good approximation for the structure even though the difference in the waveguide width at the waveguide discontinuities is large. From the result of the relative error of the modified circuit, it is assumed that the effect of higher-order modes will affect the errors because only a fundamental mode is considered in the modified circuit.

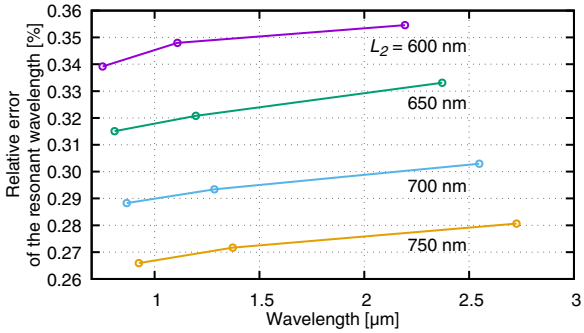

Fig. 6 The relative error of the resonant wavelength by the modified equivalent circuit to that by the FD-TD method for several lengths L_2 of the narrow waveguide. The waveguide width of the input / output and the narrow waveguide are $W_1 = W_3 = 100$ nm and $W_2 = 20$ nm, respectively.

References

[1] G. Veronis and S. Fan, "Bends and splitters in metal-dielectric-metal subwavelength plasmonic waveguides," Appl. Phys. Lett., vol.87, no.131102, pp.131102–1–3, 2005.

[2] Y. Matsuzaki, T. Okamoto, M. Haraguchi, M. Fukui, and M. Nagasaki, "Characteristics of gap plasmon waveguide with stub structures," Optics Express, vol.16, no.21, pp.16314–16325, Oct. 2008.

[3] M. Ono, H. Taniyama, H. Xu, M. Tsunekawa, E. Kuramoci, K. Nozaki, and M. Notomi, "Deep-subwavelength plasmonic mode converter with large size reduction for Si-wire waveguide," Optica, vol.3, no.9, pp.999–1005, Sep. 2016.

[4] A. Liu, R. Jones, L. Liao, D. Samara-Rubion, D. Rubin, O. Cohen, R. Nicolaescu, and M. Paniccia, "A high-speed silicon optical modulator based on a metal-oxide-semiconductor capacitor," Nature, vol.427, pp.615–618, 12 Feb. 2004.

[5] J. Liu, J. Michel, W. Giziewicz, D. Pan, K. Wada, D. Cannon, S. Jongthammanurak, D. Danielson, and L. Kimerling, "High-performance, tensile-strained Ge p-i-n photodetector on a Si platform," Appl. Phys. Lett., vol.87, p.103501, 2005.

[6] T. Tsuchizawa, K. Yamada, H. Fukuda, T. Watanabe, J. Takahashi, M. Takahashi, T. Shoji, E. Tamechika, S. Itabashi, and H. Morita, "Microphotonics devices based on silicon microfabrication technology," IEEE J. Sel. Top. Quantum Electron, vol.11, no.1, pp.232–240, Jan./Feb. 2005.

[7] J. Shibayama, Y. Wada, J. Yamauchi, and H. Nakano, "Analysis of two- and threedimensional plasmonic waveguide band-pass filters using the TRC-FDTD method," IEICE Trans. Electron., vol.E99-C, no.7, pp.817–819, July 2016.

[8] J. Shibayama, H. Kawai, J. Yamauchi, and H. Nakano, "Analysis of a 3D MIM waveguide-based plasmonic demultiplexer using the

TRC-FDTD method," Optics Communications, vol.452, pp.360–365, 2019.

[9] Y.Naka, M.Nishimoto, and M.Yokota, "Analysis of optical resonator constructed by two-dimensional MDM plasmonic waveguide," IEICE Trans. Electron., vol.E106-C, no.3, pp.103–106, 2023.

[10] A. Hosseini and Y. Massoud, "Nanoscale surface plasmon based resonator using rectangular geometry," Appl. Phys. Lett., vol.90, pp.181102–1–3, April 2007.

[11] T.B. Wang, X.W. Wen, C.P. Yin, and H.Z. Wang, "The transmission characteristics of surface plasmon polaritons in ring resonator," Optics Express, vol.17, no.26, pp.24096–24101, December 2009.

[12] F. Hu, H. Yi, and Z. Zhou, "Wavelength demultiplexing structure based on arrayed plasmonic slot cavities," Optics Letters, vol.36, no.8, pp.1500–1502, April 2011.

[13] G. Wang, H. Lu, X. Liu, D. Mao, and L. Duan, "Tunable multichannel wavelength demultiplexer based on mim plasmonic nanodisk resonators at telecommunication regime," Optics Express, vol.19, no.4, pp.3513–3518, February 2011.

[14] Y. Guo, L. Yan, W. Pan, B. Luo, K. Wen, Z. Guo, H. Li, and X. Luo, "A plasmonic splitter based on slot cavity," Optics Express, vol.19, no.15, pp.13831–13838, July 2011.

[15] K. Wen, Y. Hu, L. Chen, J. Zhou, L. Lei, and Z. Meng, "Single/dual fano resonance based on plasmonic metal-dielectric-metal waveguide," Plasmonics, vol.11, pp.315–321, 2016.

[16] Y. Chen, P. Luo, X. Liu, Y. Di, S. Han, X. Cui, and L. He, "Sensing performance analysis on fano resonance of metallic double-baffle contained MDM waveguide coupled ring resonator," Optics & Laser Technology, vol.101, pp.273–278, 2018.

[17] M.R. Rakhshani, "Optical refractive index sensor with two plasmonic double-square resonators for simultaneous sensing of human blood groups," Photonics and Nanostructures: Fundam. Appl., vol.39, p.100768, 2020.

[18] G. Veronis, Ş.E. Kocaba, D.A.B. Miller, and S. Fan, "Modeling of plasmonic waveguide components and networks," Journal of Computational and Theoretical Nanoscience, vol.6, no.8, pp.1808–1826, 2009.

[19] H. Nejati and A. Beirami, "Theoretical analysis of the characteristic impedance in metal–insulator–metal plasmonic transmission lines," Opt. Lett., vol.37, no.6, pp.1050–1052, Mar 2012.

[20] Y.Naka, M.Nishimoto, and M.Yokota, "Equivalent circuit expression of optical resonator structure constructed by two-dimensional MDM plasmonic narrow waveguide (in Japanese)," IEICE Trans. Electron. (Japanese Edition), vol.J106-C, no.9, pp.360–365, 2023.

[21] R.E. Collin, Field Theory of Guided Waves, second ed., Wiley-IEEE-Press, New York, 1991.

[22] P.B. Johnson and R.W. Christy, "Optical constants of the noble metals," Phys. Rev. B, vol.6, pp.4370–4379, 1972.

[23] D.W. Lynch and W.R. Hunter, "Comments on the optical constants of metals and an introduction to the data for several metals," Handbook of Optical Constants of Solids, ed. E.D. Palik, Boston, pp.275–367, Academic Press, 1985.

[24] D.F. Kelly and R.J. Luebbers, "Piecewise linear recursive convolution for dispersive media using FDTD," IEEE Trans. Antennas Propagat., vol.44, pp.792–797, 1996.

[25] J.P.Berenger, "A perfectly matched layer for the absorption of electromangetic waves," J. Computational Phys., vol.114, pp.185–200, 1994.

[26] T.Uno, Y.He, and S.Adachi, "Perfectly matched layer absorbing boundary condition for dispersive medium," IEEE Microwave and Guided Wave Lett., vol.7, pp.264–266, 1997.

[27] A. Pannipitiya, I.D. Rukhlenko, and M. Premaratne, "Analytical modeling of resonant cavities for plasmonic-slot-waveguide junctions," IEEE Photonics Journal, vol.3, no.2, pp.220–233, 2011.

[28] M. Bahadori, A. Eshaghian, H. Hodaei, M. Rezaei, and K. Mehrany, "Analysis and design of optical demultiplexer based on arrayed plasmonic slot cavities: Transmission line model," IEEE Photonics Technology Letters, vol.25, no.8, pp.784–786, 2013.

[29] S.A. Maier, Plasmonics: Fundamentals and Applications, Springer, New York, 2007.

[30] R.E. Collin, Foundations for Microwave Engineering, McGraw-Hill, New York, 1966.

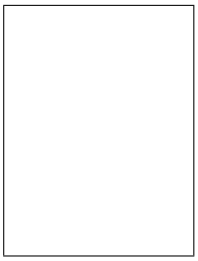

Yoshihiro NAKA received the B.E., M.E., and Ph.D. degrees in Electrical Engineering and Computer Science from Kumamoto University, Kumamoto, Japan, in 1993, 1995, and 1998, respectively. In 1998, he joined the Faculty of Engineering at Kumamoto University as a Research Associate. From 2014 to 2020, he was an Associate Professor of School of Pharmaceutical Sciences , Kyushu University of Health and Welfare. Since 2020, he has been a Associate Professor of Faculty of Engineering, University of Miyazaki. His research interests are in optical waveguides and computational electromagnetics. Dr. Naka recieved the Young Researcher's Award of IEICE Japan in 1998. He is a member of the IEEE, and the Japan Society of Applied Physics(JSAP).

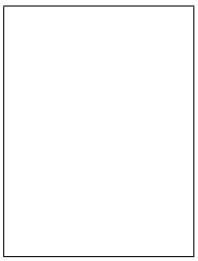

Masahiko NISHIMOTO received the B.E. degree in Electronic Engineering from Kumamoto University, Japan, in 1982, and M.E. and D.E. degrees in Computer Science and Communication Engineering, from Kyushu University, Fukuoka, Japan, in 1984 and 1987, respectively. Since 1987 he has been with a department of Electrical Engineering and Computer Science, Kumamoto University, and he is currently a professor in Faculty of Advanced Science and Technology, Kumamoto University. From 2009 to 2010, he served as IEEE AP-S Fukuoka Chapter Chair, and from 2011 to 2013, he served as the Chair of the Technical Committee on Electromagnetic Theory in Electronics Society of the IEICE. His research interests are in radar signal processing, scattering and diffraction of electromagnetic waves, and computational electromagnetics.

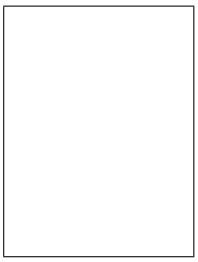

Mitsuhiro YOKOTA was born in Fukuoka, Japan, on June 25, 1959. He received the B.E., M.E., and Ph.D degrees in communication engineering from Kyushu University, Fukuoka, Japan, in 1982, 1984, and 1989, respectively. In 1986, he joined the faculty of engineering at Kyushu University. From 2005, he has been a professor of Electrical and Electronic Engineering at Miyazaki University. His research interests are in electromagnetic wave theory and numerical analysis. He received the award of the best presentation of the paper from the Institute of Electrical Engineers of Japan in 1991. Dr. Yokota is a senior member of the IEICE, and a member of the IEEE, the IEEJ, and OSA.